THERMAL, MECHANICAL AND WATER SORPTION PROPERTIES OF XANTHAN-BASED COMPOSITE CRYOGELS

IRINA ELENA RASCHIP,[*] MARIA VALENTINA DINU,[*] NICUSOR FIFERE,[*] RALUCA DARIE-NITA,[*] DANIELA PAMFIL,[*] ANDREEA POPIRDA[*,**] and CRISTIAN LOGIGAN[***]

[*] *"Petru Poni" Institute of Macromolecular Chemistry, 41A, Grigore Ghica Voda Alley, Iasi 700487, Romania*
[**] *"Ion Ionescu de la Brad" University of Agricultural Sciences and Veterinary Medicine, Iasi, Romania*
[***] *Chemical Company SA, 14, Chemistry Boulevard, Iasi 707252, Romania*
✉ *Corresponding author: Maria Valentina Dinu, vdinu@icmpp.ro*

Received April 30, 2020

The thermal, mechanical, rheological, and surface characteristics of some xanthan/poly(vinyl alcohol)/red grape pomace composite cryogels prepared by the freeze/thawing approach were investigated. The results were discussed in comparison with those obtained for individual xanthan or poly(vinyl alcohol) cryogel networks synthesized under the same conditions. The mechanical strength of the cryogels was enhanced by increasing the number of freeze/thawing cycles, and by the addition of a natural polyphenol (*i.e.* red grape pomace). The thermal stability of the poly(vinyl alcohol) in the blend significantly decreased upon the addition of 50% xanthan, while the presence of a single neat melting profile indicated good component miscibility for the chosen ratios. The water sorption capacity depended on the amount of polyphenol incorporated, thus the hydrophilicity of the cryogel films decreased with the increase of polyphenol content.

Keywords: xanthan-based films, thermostability, mechanical properties, water sorption behavior

INTRODUCTION

Polysaccharide-based hydrogels are 3D macromolecular networks obtained from natural polymers capable to accommodate significant amounts of water, without undergoing dissolution due to the presence of physical or chemical cross-links.[1,2] The ability to mimic body tissues and to respond to external stimuli recommend them as important and promising forms of biomaterials for large-scale applications in both biomedical and pharmaceutical fields.[1,2] However, they exhibit poor mechanical strength and a slow response rate to an external stimulus, such as pH, temperature, ionic strength, light, electric and magnetic field, or a combination of them. Consequently, studies on composite materials have aroused great interest, since they are endowed with enhanced thermal, mechanical, swelling, permeation, optical, surface or antibacterial characteristics.

Lately, composite hydrogels based on chitosan, salecan, pullulan, alginate, and xanthan gum (XG), with a wide range of micro-morphologies and properties, have been designed[3-12] by various strategies, including blending with other natural or synthetic polymers, cryogelation, or embedding of clay minerals. Polysaccharide-based composites are attractive biomaterials for biomedical, biotechnological and environmental applications, as drug delivery systems,[3,4] scaffolds,[5-7] packaging materials,[8,9] sensors,[10] and adsorbents of various pollutants from wastewaters.[11-14]

Among polysaccharides, XG is an important water-soluble anionic natural polymer that has been used widely in various applications, starting from medicine and food industry to wastewater treatment.[15-18] To obtain superabsorbent XG-based composite hydrogels, interpenetrating polymer networks have been prepared by selective cross-linking of one polymer (XG, lignin, poly(acrylic acid) or poly(vinyl alcohol)) in a polymer blend.[15-21] By embedding halloysite nanotubes and cellulose nanocrystals within sodium alginate/XG matrices, nanocomposite scaffolds with reinforced mechanical properties have been engineered,[22] while the incorporation of montmorillonite into XG/2-arylamido-2-methyl-1-propane sulfonic acid hydrogel networks led to efficient organic–inorganic composite sorbents.[23] The water diffusion properties of XG-based hydrogels have been improved by engineering porous matrices using the cryogelation technique.[24,25]

Cryogelation is a versatile and eco-friendly method in which the cross-linking polymerization reactions are conducted below the freezing point of the reaction mixture.[26] In this approach, the ice crystals act as a template that, after thawing, leaves networks with highly interconnected pores known as cryogels. Cryogel-based materials have potential applications in the field of bioseparation, medicine and wastewater treatment.[26-28] However, the production of previously reported porous polysaccharide-based materials required the embedding of some toxic monomers or chemical cross-linkers to construct the gel skeleton, which reduced their potential usage within clinical practice.[12,29,30]

Physically cross-linked salecan-based hydrogels have been recently obtained by blending salecan with κ-carrageenan[6] or curdlan.[7] In this respect, the objective of this work was to develop a series of XG-based cryogels, without the addition of supplementary toxic cross-linkers or synthetic monomers. Thus, physically cross-linked XG/poly(vinyl alcohol) (PVA) cryogel films embedding a natural polyphenol, *i.e.* red grape pomace (RGP), were successfully produced by the association of the functional groups of XG, PVA, and polyphenol through hydrogen bonds. The optimum reaction conditions to prepare these materials have been successfully identified previously.[25] Better comprehension of the structure/property relationship is essential since these cryogel composites are intended to meet the particular requirements of packaging materials. Therefore, in this study, the XG/PVA cryogel films, with or without RGP, were further characterized by thermogravimetry (TG), differential scanning calorimetry (DSC), uniaxial compression tests, dynamic rheology, dynamic water vapor sorption (DVS), swelling, and contact angle (θ) measurements. The thermostability, mechanical properties and water sorption properties of the XG/PVA composite cryogels were systematically investigated in comparison with those of the individual XG or PVA network.

EXPERIMENTAL

Materials

Xanthan gum (XG), as powder, with an average molecular weight of 1980 kg mol^{-1}, was purchased from Aldrich. Poly(vinyl alcohol) (PVA), with an average molecular weight of 89,000-98,000 g mol^{-1} and a hydrolysis degree of 99%, was also purchased from Aldrich. The red grape pomace (RGP) sample resulted from the process of wine preparation and was provided by "Ion Ionescu de la Brad" University of Agricultural Sciences and Veterinary Medicine. The RGP was used as a reinforcing agent within XG-based cryogel films, and the main natural component determined by HPLC in this sample was resveratrol.

Preparation of cryogel films

The composite cryogel films based on XG, PVA, and RGP were prepared by the freeze/thawing methodology using the previously reported protocols.[25] Briefly, polymeric solutions of XG and PVA, with or without embedded RGP, were transferred to standard weighing bottles and were subjected to several freeze/thawing cycles. The freeze/thawing conditions per each cycle were kept constant for all the samples, as follows: freezing temperature: –20 °C; freezing time: 24 h; thawing temperature: 22 °C, and thawing time: 12 h. The weight ratio between XG and PVA was 50:50 or 75:25, while the weight ratio between RGP and the polymeric components was 0.2:1 or 0.5:1. The sample codes include the abbreviations of polymeric compounds, the wt% of XG, the number of the freeze/thawing cycles, and the amount of RGP where it was the case. For example, XG50PVA3.AO0.2 represents the code for the composite films obtained with a weight ratio between XG and PVA of 50:50, in 3 freeze/thawing cycles with 0.2 wt% of RGP. Before characterization, all the samples were freeze-dried in a LABCONCO FreeZone device for 24 h, at –48 °C and 0.05 mbars.

Characterization methods

Thermogravimetric analysis (TGA) was performed on a STA 449F1 Jupiter device (Netzsch-Germany). 15 mg of each sample was heated up to 700 °C under N_2 gas, at a flow rate of 50 mL min^{-1}, in an open Al_2O_3 crucible.

Differential scanning calorimetry (DSC) measurements were conducted on a DSC 200 F3 Maia device (Netzsch, Germany). Approximately 10 mg of sample was heated in closed aluminum crucibles. Experiments were conducted under N_2 purge at a flow rate of 50 mL min^{-1} and a heating rate of 10 °C min^{-1}. The instrument was calibrated with indium according to standard procedures.

Uniaxial compression measurements on XG-based hydrogels were performed using a mechanical tester (Shimadzu Testing Machine EZTest equipped with a 500 N load cell), at a compression rate of 1 mm min^{-1} up to 80% strain. This test was applied on circular rods, freshly freeze/dried samples of 50 mm in diameter and 5 mm in length. The setup of the test and calculations of compressive strength and modulus were performed in accordance with previously published reports in the field of polysaccharide-based hydrogels.[25,31] Compressive

strength was determined as the compressive stress at 10% strain, while the modulus was calculated as the gradient of the initial linear portion in the stress-strain curve.

Dynamic rheology tests were performed on a Physica MCR 301 rheometer (Anton Paar, Austria) with parallel-plate geometry (upper diameter of 25 mm) and a fixed gap of 1 mm. Oscillatory frequency sweep tests were performed in the frequency domain between 0.05 and 500 rad/s, with a previously determined fixed strain of 5% in the linear viscoelastic region (LVE). Each freshly prepared sample was placed in the center of the rheometer plate in dried state, being hydrated (1.5%) with MilliQ water before the rheological measurements. The test geometry was lowered to the desired gap height and excess hydrogel was removed, so that the hydrogel correctly filled the geometry. In order to prevent water evaporation, the rheological measurements were conducted at constant temperature (25 ± 0.1 °C), using a Peltier system for control of temperature and evaporation, so constant sample hydration was kept during testing.

Dynamic water vapor sorption (DVS) was measured using an IGAsorp gravimetric analyzer (Hiden Analytical, Warrington (UK)), according to a protocol applied for dextran-based cryogels.[32] The experimental data were recorded at 25 °C and a relative humidity (RH) ranging from 0 to 90%.

The ***static water swelling behavior*** of XG/PVA cryogels obtained under freeze/thawing conditions was gravimetrically studied at RT. The swelling ratio (SR, g g^{-1}) was calculated by Equation 1:[25]

$$SR = \frac{mt}{md}, \text{ g g}^{-1} \quad (1)$$

where m_t and m_d are the weights of the samples at time t and in dry state.

Static contact angle (θ) measurements for the obtained materials were evaluated using the sessile drop method at RT after placing 1 μL drop of liquid on the film surface, using a CAM-200 instrument from KSV, Finland. The Young–Laplace equation was used for fitting the drop profile on the surface of each sample, as described previously.[20] All the measurements were done five times and the acquired data were expressed as average values ± standard deviations.

RESULTS AND DISCUSSION

The XG-based cryogel composites, as films, were successfully prepared by cryogenic gelation through several freeze/thawing cycles. Information about the features of the XG/PVA composite cryogels was obtained by evaluation of their thermal stability, mechanical properties, and static and dynamic water swelling behavior, in comparison with those of the hydrogel matrix based only on XG or PVA. The stability of the XG/PVA cryogel films is not based on the homogeny distribution of the intermolecular hydrogen bonds, but rather on the crystalline zones created by PVA under the freeze/thaw treatment. These zones are ordered structures acting as junction knots, leading to a network where the intermolecular hydrogen bonds based on -OH and -COOH groups has the highest density. The network based on crystalline junction knots represents a physical cross-linking, where the interaction between XG and PVA can be also realized by intermolecular entanglement. To get deeper insights into the structure/property relationships of the XG/PVA composite cryogels, their thermostability, mechanical strength, and water sorption properties were systematically investigated in comparison with those of the individual XG or PVA network.

Thermogravimetric analysis

The thermal degradation behavior of the XG/PVA cryogels, with and without RGP impregnation, was compared with the thermal behavior of the raw XG and PVA, respectively. Thermogravimetric curves, TG, and differential weight loss curves, DTG and DSC, are shown in Figure 1. Figure 1 presents the TGA curves, their corresponding first derivatives (DTG) and second DSC scans of the studied structures. Some thermogravimetric characteristics are shown in Table 1.

XG loses 15% humidity in the range 65-125 °C, due to its polar groups, especially the –OH ones, and thermally decomposes in a single stage, in the temperature range 246-310 °C, with a mass loss of 54% and a residue value of 30.95%. This is in good agreement with the thermal data reported for other polysaccharides.[33,34] The presence of 50% XG significantly decreases the thermal stability of PVA in the blend (XG50PVA3 sample) in the temperature range 240-483 °C, comparable to that of pure XG, however, it induces a much lower total mass loss (67.7%) than that of PVA and a much higher residue value (23.86%), with comparable water loss (8.3%).

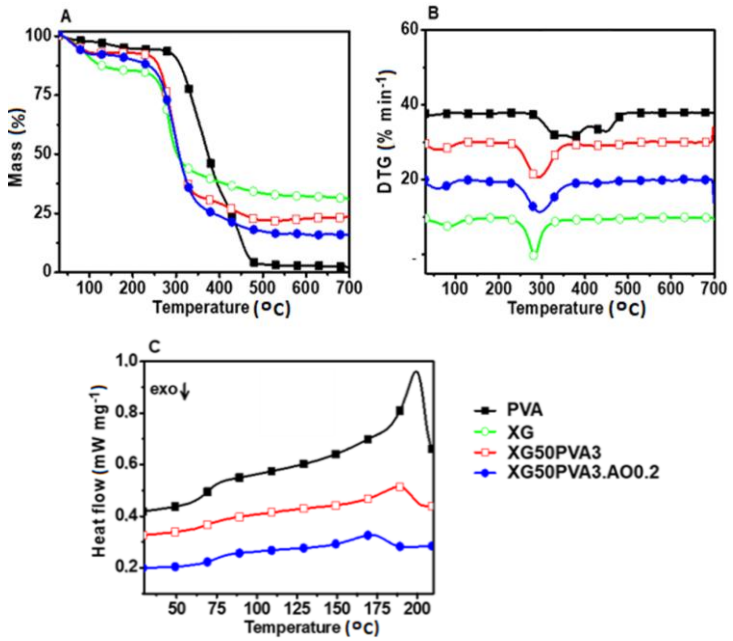

Figure 1: TGA (A), DTG (B) and DSC (C) curves of PVA, XG and of XG/PVA cryogels without (XG50PVA3) and with RGP (XG50PVA3.AO0.2)

Table 1
Thermogravimetric characteristics of XG/PVA cryogels

Sample		TGA					DSC		
	Stage	T_{onset} (°C)	T_{max} (°C)	T_{endset} (°C)	W_m (%)	W_{rez} (%)	T_g (°C)	T_m (°C)	ΔH_m (J g^{-1})
XG3	I	65	84	125	15		–	–	–
	II	246	283	310	54	30.95			
PVA3	I	50	35	195	6.16		70	200	36.85
	II	290	329	400	64.39				
	III	423	449	473	27.2	2.06			
XG50PVA3	I	37	61	100	8.3		72	189	12.41
	II	240	292	338	60.76				
	III	390	425	483	6.95	23.86			
XG50PVA3.AO0.2	I	36	63	98	7.14		75	168	7.06
	II	160	295	346	67.1				
	III	410	413	493	9.2	15.68			

T_{onset} – onset temperature of thermal degradation; T_{max} – temperature that corresponds to the maximum rate of thermal decomposition for each stage evaluated from the peaks of the DTG curves; T_{endset} – endset temperature of thermal degradation; W_m – mass loss rate corresponding to each thermal degradation stage; W_{rez} – percentage of residue remaining at the end of thermal degradation (700 °C); T_g – glass transition temperature; T_m – melting temperature; ΔH_m – melting enthalpy

Also, by analyzing the DTG curves of PVA, XG and their blends (XG50PVA3 and XG50PVA3.AO0.2 samples) (Fig. 1B), one may observe that for the latter two the first two DTG peaks merge and the third DTG curve peak almost disappears. The samples tend to behave like pure XG, as a single system, thus this element ratio generates good miscibility between the components. The addition of RGP (XG50PVA3.AO0.2 sample) generates similar thermal degradation behavior, except for significantly lowering the thermal stability temperature range (160-493 °C) and reducing mass residue (15.68%). Figure 1C shows the second DSC scans, after previous sample thermal history removal, amongst which the pure XG exhibited a wide dehydration endotherm. By analyzing Figure 1C and Table 1, it may be seen that PVA exhibits a typical glass transition temperature domain (T_g) centered at 70 °C, a melting profile (T_m) at 200 °C, with an enthalpy (ΔH_m) value of 36.85 J g^{-1}. The addition of XG and RGP to the blend leads to a slight increase in T_g values to 72 °C and 75 °C, respectively. This means that specific interactions occur between system components through

hydrogen bonds. Moreover, this aspect also leads to a significant decrease of T_m and ΔH_m values to 189 °C and 12.41 J g^{-1} (XG50PVA3 sample), and 168 °C, and 7.06 J g^{-1} (XG50PVA3.AO0.2 sample). Nonetheless, the presence of a single neat melting profile indicates good component miscibility for the chosen ratios, as compared to other systems,[35,36] thus being in good agreement with the thermal decomposition data.

Mechanical properties

Unconfined compression tests were performed on lyophilized samples, in order to investigate the effect of the entrapment of PVA or RGP within the XG matrices on the mechanical performances. Typical stress-strain compression curves are presented in Figure 2.

The elastic modulus of all the hydrogels was determined from the slope of the linear dependence of the stress-strain curves (Fig. 2B) and the data obtained were summarized in Table 2.

As can be seen from the compression stress-strain curves recorded for the XG/PVA cryogels, the addition of PVA imparts greater elasticity to the polymer films. However, the incorporation of RGP into the XG/PVA matrix induced stiffening of the films. This stiffening was also observed when the number of freeze/thawing cycles increased from 3 to 7 (Fig. 3). An enhancement of the stiffness of the XG-based hydrogels, in dry state, has been also reported for XG-based hybrid scaffolds when silica glass was incorporated into an XG matrix.[37]

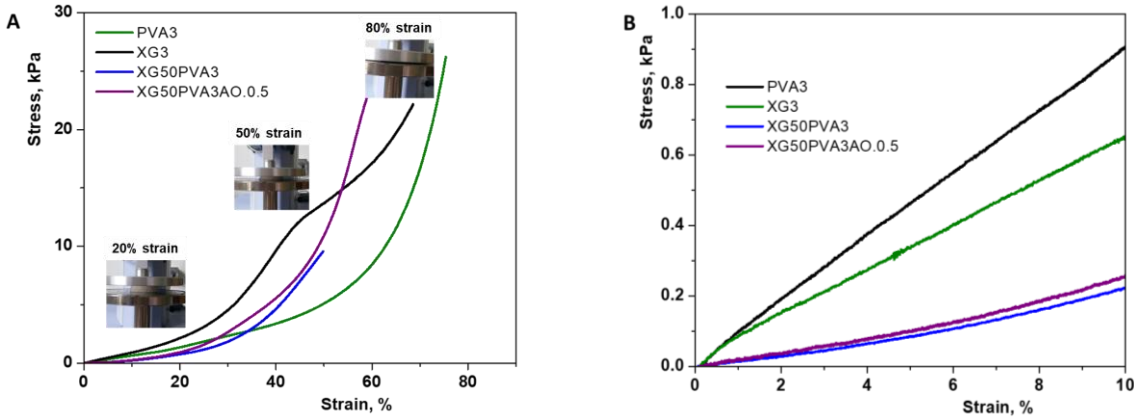

Figure 2: (A) Representative compression stress-strain curves for XG/PVA cryogels obtained in three freeze/thawing cycles under uniaxial compression (optical pictures from the insets correspond to XG50PVA3 sample); (B) Linear dependence of stress-strain curves from which the elastic moduli of all composites were calculated

Table 2

Elastic modulus values of lyophilized XG-based composite hydrogels in comparison with those of XG and PVA cryogels prepared after 3 freeze/thawing cycles

Sample code	Freeze/thawing cycles	XG	PVA	RGP content, w/w%	Elastic modulus, kPa	R^2
XG3	3	100	0	0	0.98	0.996
PVA3	3	0	100	0	0.65	0.999
XG50PVA3	3	50	50	0	0.31	0.963
XG50PVA3.AO.0.5	3	50	50	0.5	0.39	0.952

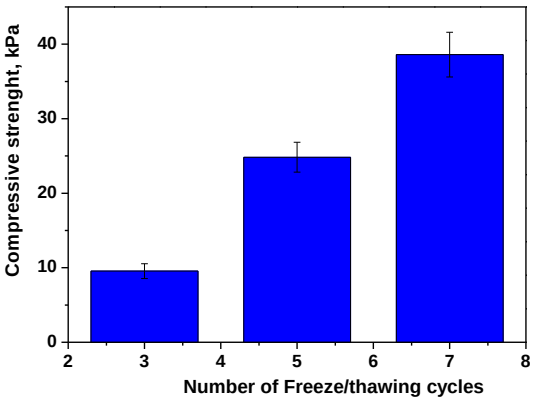

Figure 3: Compressive strength of RGP containing XG/PVA cryogels as a function of the number of freeze/thawing cycles

The XG/PVA cryogels containing 0.5 w/w% of RGP (Fig. 3), prepared using 3, 5 and 7 freeze/thawing cycles, exhibited a compressive strength of about 9, 25, and 38 kPa, respectively. The values of compressive strength increased with the increase in the number of the freeze/thawing cycles due to the high degree of the reinforcement determined by the microcrystalline network of PVA, which led to more cross-linked networks through hydrogen bonds. An enhancement of the compressive moduli has been also reported for κ-carrageenan/salecan hydrogels, as the ratio of κ-carrageenan to salecan increased, being attributed to the formation of more physical junctions through van der Waals forces, such as hydrogen bonds.[7]

The effect of the number of freeze/thawing cycles on the mechanical properties of the XG/PVA cryogels was also evaluated by rheology. Rheological studies offer important information on the viscoelastic behavior of materials. Dynamic storage modulus (G') represents the ability to accumulate and release energy during the application of deformations (elastic behavior of material), and the modulus of loss (G") is a measure of dissipated energy and refers to the viscous nature of the material. The evolution of the dynamic modulus presented in Figure 4 demonstrates the increase of G' and G", both with the frequency and with the number of freeze/thawing cycles.

A strong dependence of the dynamic moduli G' and G" as a function of angular frequency was observed. An increase in the G' and G" values was noticed when increasing the oscillation frequency, because at low frequencies there is enough time for the chains to unfold, so they relax slowly. When the polymer chains were deformed at high frequencies, the entangled chains did not have enough time to reorient, leading to an increase of the moduli. For the experiments carried out in LVE at $\omega = 0.1\ s^{-1}$, where G' > G" for the whole experimental domain, it was observed that if G' > 10 Pa, a certain stability of the hydrogel can be assumed.[38] The results obtained from the rheological tests in dynamic mode also show the effect of the ratio between the components on the rheological behavior of the XG matrix hydrogel (Fig. 5 and Table 3).

The graphs shown in Figure 5 reveal that the presence of PVA in the XG matrix led to a decrease in the resistance of the hydrogel (G') at low oscillation frequencies (~0.1-10 s^{-1}) – the gels became softer, but maintained their stable structure.

The complex dynamic viscosity decreases with increasing oscillation frequency for all the materials. Higher viscosity values were recorded when RGP was incorporated into the XG75PVA7 cryogel films.

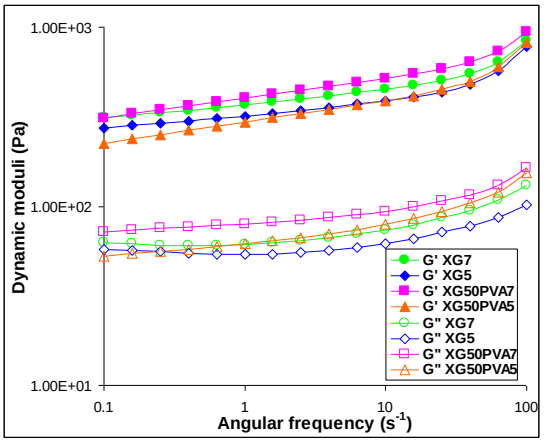

Figure 4: Influence of freeze/thawing cycles on the variation of storage modulus (G′) and loss modulus (G″) as a function of angular oscillation frequency at 25 °C for XG and systems containing 50% XG

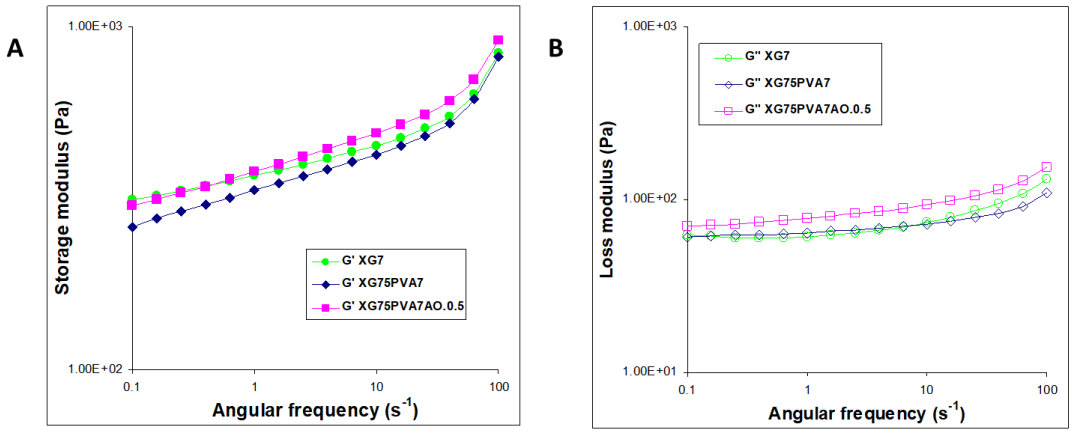

Figure 5: Variation of (a) storage modulus (G′) and (b) loss modulus (G″) as a function of angular oscillation frequency at 25 °C for systems containing 75% XG after 7 freeze/thawing cycles

Table 3
Complex dynamic viscosity (|η*|) dependence on angular frequency (ω) for xanthan matrix and hydrogels containing 75% XG after 7 freeze/thawing cycles

ω (s^{-1})	|η*| (Pa.s)		
	XG7	XG75PVA7	XG75PVA7AO.0.5
0.1	3190	2680	3090
1	373	340	386
10	45.6	43.1	49.8
100	8.49	8.4	9.24

Water sorption properties

Since these biomaterials are intended for use in the food packaging industry, it is important to assess their properties under different humidity conditions. Thus, the DVS and static swelling behavior of these XG/PVA cryogels were determined (Fig. 6).

The weight changes with the change of RH were measured in the analysis chamber at 25 °C, using a microbalance. The sorption–desorption isotherms corresponding to the XG/PVA cryogels are shown in Figure 6. According to the IUPAC classification, the isotherms obtained for all the XG/PVA cryogels prepared in the present study (Fig. 6) correspond to type V, indicating the presence of a porous structure. Furthermore, the DVS sorption data were used to estimate the BET_{H2O} surface,[32,39,40] the values obtained being presented in Table 4.

The incorporation of RGP leads to changes in both the BET_{H2O} surface and the water retention capacity (Table 4). The XG50PVA3 cryogels have the largest BET_{H2O} surface and water retention capacity, because these parameters are significantly influenced by the morphology and composition of

the materials. The DVS are well correlated with the static swelling behavior of these XG/PVA cryogels (Fig. 6B). The XG/PVA cryogels showed a swelling behavior characteristic of macroporous morphologies with interconnected pores.[25] The XG/PVA cryogels without RGP attained the swelling equilibrium in 8 min and those containing RGP – within about 20 min. The incorporation of RGP within the XG/PVA network conducted to a decrease in the swelling ratio (Fig. 6B), which could be associated with the decrease in the hydrophilicity of the films upon RGP addition.

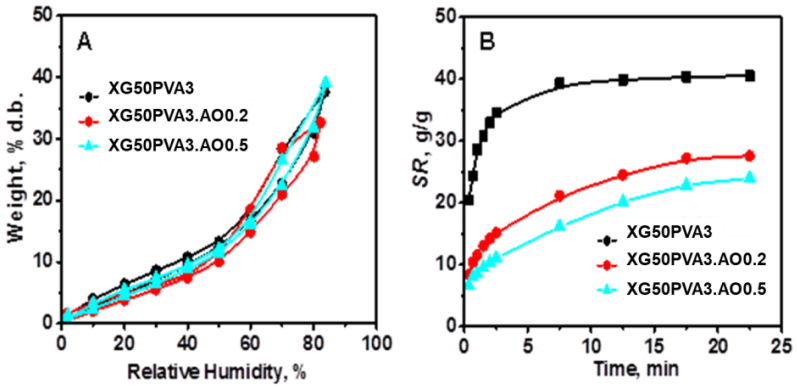

Figure 6: (A) Sorption and desorption isotherms of XG/PVA cryogels prepared using an XG:PVA ratio of 50:50, through 3 freeze/thawing cycles, without RGP (XG50PVA3) and with RGP content of 0.2 wt% (XG50PVA3.AO0.2), and, respectively, of 0.5 wt% (XG50PVA3.AO0.5); (B) Swelling ratio (SR, g/g) of XG/PVA cryogels as a function of time (min)

Table 4
Dynamic water vapor sorption data of XG/PVA cryogels prepared using an XG:PVA ratio of 50:50, through 3 freeze/thawing cycles

Sample	Weight, % d.b.	BET_{H2O}	
		Surface, m^2/g	Multilayer, g/g
XG50PVA3	37.604	273.120	0.061
XG50PVA3.AO.0.2	32.016	195.24	0.074
XG50PVA3.AO.0.5	29.502	182.45	0.095

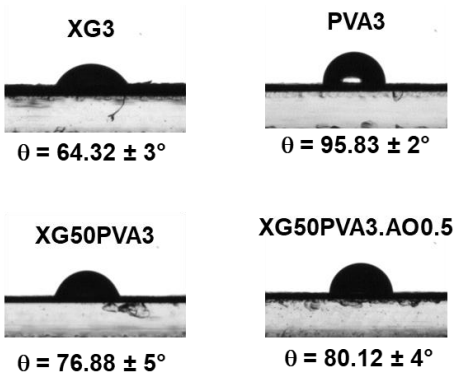

Figure 7: Water contact angle values corresponding to XG-based cryogel films

Bueno and collaborators[41] studied the swelling mechanism of XG-based hydrogels by tensiometry. It was shown that the initial water uptake mechanism is associated with fast diffusion of the solvent through the interconnected pores, without interaction with polymeric chains, which also applies to the materials developed in our study. However, the swelling mechanism of XG-based hydrogels has changed from Fickian diffusion (water diffusion does not depend on chain relaxation) to anomalous (there is interaction between diffusive water and polymeric chains) with the presence of citric acid, as cross-linker.[41] By applying the equation proposed by Krosmeyer and Peppas to our experimental swelling data, it was found that the pseudo-Fickian diffusion is the main transport mechanism responsible for the swelling of the XG-based cryogels, in which the polymer chain relaxation is

negligible during sorption. The water contact angle of the XG-based cryogel films was also measured, and the results are shown in Figure 7.

Following the assessment of the water contact angle between the surface of the samples and the water drop (Fig. 7), high hydrophilicity was revealed for the XG3 cryogel film. The addition of PVA or RGP reduced the hydrophilicity of the network (higher values of the water contact angle), which are consistent with the results of the static swelling measurements.

CONCLUSION

By incorporation of PVA, RGP or by increasing the number of freeze/thawing cycles, the thermal, mechanical, rheological, and surface characteristics of XG-based cryogel films could be varied. The thermal stability in the blend was not significantly affected by RGP addition, but it decreased upon XG incorporation. The values of compressive strength increased with the increase of the number of the freeze/thawing cycles. Thus, the XG/PVA cryogels containing 0.5 w/w% of RGP prepared using 3, 5 and 7 freeze/thawing cycles exhibited a compressive strength of about 9, 25, and 38 kPa, respectively. The BET_{H2O} surface, the water retention capacity, and the water contact values depended on the amount of RGP embedded within the XG/PVA cryogels. The samples prepared with the highest RGP content showed the lowest water sorption capacity. Our results point out that green physically cross-linked XG/PVARGP cryogels, with improved thermal, mechanical, and surface properties, could be easily developed by cryogelation, allowing to envisage some future applications for these composites as food packaging materials, controlled drug delivery systems, and tissue engineering scaffolds.

ACKNOWLEDGMENTS: This work was supported by a grant of the Romanian Ministry of Research and Innovation (CCCDI-UEFISCDI) PN-III-P1-1.1-TE-2016-2038 project [TE77/10.10.2018]. The European Social Fund for Regional Development, Competitiveness Operational Programme Axis 1 – Project "Petru Poni Institute of Macromolecular Chemistry – Interdisciplinary Pole for Smart Specialization through Research and Innovation and Technology Transfer in Bio(nano)polymeric Materials and (Eco)Technology", InoMatPol (ID P_36_570, Contract 142/10.10.2016, code MySMIS: 107464) is also acknowledged.

REFERENCES

[1] V. K. Thakur and M. K. Thakur, *J. Clean Prod*., **82**, 1 (2014), https://doi.org/10.1016/j.jclepro.2014.06.066
[2] N. Sood, A. Bhardwaj, S. Mehta and A. Mehta, *Drug Deliv*., **23**, 748 (2016), https://doi.org/10.3109/10717544.2014.940091
[3] X. Tong, W. Pan, T. Su, M. Zhang, W. Dong *et al*., *React. Funct. Polym*., **148**, 104501 (2020), https://doi.org/10.1016/j.reactfunctpolym.2020.104501
[4] E. S. Dragan and M. V. Dinu, *Carbohyd. Polym*., **225**, 115210 (2019), https://doi.org/10.1016/j.carbpol.2019.115210
[5] T. Zhu, J. Mao, Y. Cheng, H. Liu, L. Lv *et al*., *Adv. Mater. Interfaces*, **6**, 1900761 (2019), https://doi.org/10.1002/admi.201900761
[6] X. Qi, M. Zhang, T. Su, W. Pan, X. Tong *et al*., *J. Agric. Food Chem*., **68**, 3770 (2020), https://doi.org/10.1021/acs.jafc.9b06120
[7] X. Qi, T. Su, M. Zhang, X. Tong, W. Pan *et al*., *ACS Appl. Mater. Interfaces*, **12**, 13256 (2020), https://doi.org/10.1021/acsami.9b20794
[8] P. Cazon, G. Velazquez, J. A. Ramirez and M. Vazquez, *Food Hydrocoll*., **68**, 136 (2017), https://doi.org/10.1016/j.foodhyd.2016.09.009
[9] N. Kumar, Neeraja, A. Ojha and R. Singh, *React. Funct. Polym.*, **144**, 104350 (2019), https://doi.org/10.1016/j.reactfunctpolym.2019.104350
[10] W. Suginta, P. Khunkaewla and A. Schulte, *Chem. Rev*., **113**, 5458 (2013), https://doi.org/10.1021/cr300325r
[11] X. Qi, M. Chen, Y. Qian, M. Liu, Z. Li *et al*., *Int. J. Biol. Macromol*., **132**, 429 (2019), https://doi.org/10.1016/j.ijbiomac.2019.03.155
[12] M. V. Dinu, I. A. Dinu, M. M. Lazar and E. S. Dragan, *Cellulose Chem. Technol*., **52**, 181 (2018), https://www.cellulosechemtechnol.ro/pdf/CCT3-4(2018)/p.181-192.pdf
[13] N. Cankaya and R. Sahin, *Cellulose Chem. Technol*., **53**, 537 (2019), https://doi.org/10.35812/CelluloseChemTechnol.2019.53.54
[14] M. Râpă, E. Matei, A. Țurcanu, A. M. Predescu, M. C. Pantilimon *et al*., *Cellulose Chem. Technol*., **53**, 561 (2019), https://doi.org/10.35812/CelluloseChemTechnol.2019.53.56

[15] I. E. Raschip, E. G. Hitruc, A. M. Oprea, M. C. Popescu and C. Vasile, *J. Mol. Struct.*, **1003**, 67 (2011), https://doi.org/10.1016/j.molstruc.2011.07.023
[16] A. Kumar, K. M. Rao and S. S. Han, *Carbohyd. Polym.*, **180**, 128 (2018), https://doi.org/10.1016/j.carbpol.2017.10.009
[17] D. F. S. Petri, *J. Appl. Polym. Sci*., **132**, 42035 (2015), https://doi.org/10.1002/app.42035
[18] Z. Zhao, C. Zhou, X. Zhang and Y. Zhang, *Environ. Prog. Sustain.*, **33**, 430 (2014), https://doi.org/10.1002/ep.11802
[19] I. E. Raschip, G. E. Hitruc, C. Vasile and M. C. Popescu, *Int. J. Biol. Macromol.*, **54**, 230 (2013), https://doi.org/10.1016/j.ijbiomac.2012.12.036
[20] I. E. Raschip, O. M. Paduraru-Mocanu, L. E. Nita and M. V. Dinu, *J. Appl. Polym. Sci.*, **137**, 49111 (2020), https://doi.org/10.1002/app.49111
[21] S. S. Bhattacharya, A. Mishra, D. Pal, A. K. Ghosh, A. Ghosh *et al*., *Polym. Plast. Technol*., **51**, 878 (2012), https://doi.org/10.1080/03602559.2012.671421
[22] A. Kumar, K. M. Rao and S. S. Han, *Polym. Test.*, **63**, 214 (2017), https://doi.org/10.1016/j.polymertesting.2017.08.030
[23] M. A. Jalalia, A. D. Koohia and M. Sheykhan, *Carbohyd. Polym.*, **142**, 124 (2016), https://doi.org/10.1016/j.carbpol.2016.01.033
[24] Q. Zhang, X. M. Hu, M. Y. Wu, M. M. Wang, Y. Y. Zhao *et al*., *React. Funct. Polym.*, **136**, 34 (2019), https://doi.org/10.1016/j.reactfunctpolym.2019.01.002
[25] I. E. Raschip, N. Fifere, C.-D. Varganici and M. V. Dinu, *Int. J. Biol. Macromol*., **156**, 608 (2020), https://doi.org/10.1016/j.ijbiomac.2020.04.086
[26] V. I. Lozinsky, *Russ. Chem. Rev*., **71**, 489 (2002), https://doi.org/10.1070/RC2002v071n06ABEH000720
[27] G. G. de Lima, F. Traon, E. Moal, M. Canillas, M. A. Rodriguez *et al*., *Polym. Compos*., **39**, E210 (2017), https://doi.org/10.1002/pc.24450
[28] S. Akgönüllü, M. Bakhshpour, N. İdil, M. Andaç, H. Yavuz *et al*., *Hacettepe J. Biol. Chem*., **48**, 99 (2020), https://doi.org/10.15671/hjbc.629355
[29] X. Qi, W. Wei, J. Shen and W. Dong, *J. Mater. Chem. B*, **7**, 2577 (2019), https://doi.org/10.1039/C8TB03312A
[30] W. Wei, X. Qi, J. Li, G. Zuo, W. Sheng *et al*., *ACS Biomater. Sci. Eng*., **2**, 1386 (2016), https://doi.org/10.1021/acsbiomaterials.6b00318
[31] D. M. Suflet, I. M. Pelin, M. V. Dinu, M. Lupu and I. Popescu, *Cellulose Chem. Technol*., **53**, 897 (2019), https://doi.org/10.35812/CelluloseChemTechnol.2019.53.87
[32] M. V. Dinu, M. Cazacu and E. S. Drăgan, *Cent. Eur. J. Chem*., **11**, 248 (2013), https://doi.org/10.2478/s11532-012-0155-6
[33] M. J. Zohuriaan and F. Shokrolahi, *Polym. Test.*, **23**, 575 (2004), https://doi.org/10.1016/j.polymertesting.2003.11.001
[34] S. Faria, C. L. de Oliveira Petkowicz, S. A. L. de Morais, M. G. H. Terrones, M. M. de Resende *et al*., *Carbohyd. Polym.*, **86**, 469 (2011), https://doi.org/10.1016/j.carbpol.2011.04.063
[35] E. Fathi, N. Atyabi, M. Imani and Z. Alinejad, *Carbohyd. Polym*., **84**, 145 (2011), https://doi.org/10.1016/j.carbpol.2010.11.018
[36] C.-D. Varganici, O. M. Paduraru, L. Rosu, D. Rosu and B. C. Simionescu, *J. Anal. Appl. Pyrol*., **104**, 77 (2013), https://doi.org/10.1016/j.jaap.2013.09.004
[37] A. Kumar, K. M. Rao, S. E. Kwon, Y. N. Lee and S. S. Han, *Mater. Lett*., **193**, 274 (2017), https://doi.org/10.1016/j.matlet.2017.01.143
[38] C. Ibănescu, M. Danu, A. Nanu, M. Lungu and B. C. Simionescu, *Rev. Roum. Chim.*, **55**, 933 (2010), http://revroum.lew.ro/wp-content/uploads/2010/RRCh_11-12_2010/Art%2022.pdf
[39] S. L. Wang, C. T. Johnston, D. L. Bish, J. L. White and S. L. Hem, *J. Colloid Interface Sci*., **260**, 26 (2003), https://doi.org/10.1016/S0021-9797(02)00150-9
[40] L. Czepirski, E. Komorowska-Czepirska and J. Szymońska, *Appl. Surf. Sci.*, **196**, 150 (2002), https://doi.org/10.1016/S0169-4332(02)00050-8
[41] V. B. Bueno, R. Bentini, L. H. Catalani and D. F. S. Petri, *Carbohyd. Polym.*, **92**, 1091 (2013), https://doi.org/10.1016/j.carbpol.2012.10.062